Articles

Synthesis and Structure−Activity Relationship Effects on the Tumor Avidity of Radioiodinated Phospholipid Ether Analogues

Anatoly N. Pinchuk,[†,‡,#] Mark A. Rampy,[†] Marc A. Longino,[†,‡,#] R. W. Scott Skinner,[§] Milton D. Gross,[§] Jamey P. Weichert,*[,||,‡,#] and Raymond E. Counsell[†]

Department of Pharmacology, The University of Michigan Medical School, 1301 MSRB III, 1150 W. Medical Center Drive, Ann Arbor, Michigan 48109-0632, the Nuclear Medicine Service, VA Medical Center, 2215 Fuller Road, Ann Arbor, Michigan 48105-2303, Department of Radiology, University of Michigan Medical School, Ann Arbor, Michigan, 48109-0030, and Department of Radiology, University of Wisconsin Medical School, E3 Clinical Science Center, 600 Highland Avenue, Madison, Wisconsin 53792-3252

Received March 18, 2005

Radioiodinated phospholipid ether analogues have shown a remarkable ability to selectively accumulate in a variety of human and animal tumors in xenograft and spontaneous tumor rodent models. It is believed that this tumor avidity arises as a consequence of metabolic differences between tumor and corresponding normal tissues. The results of this study indicate that one factor in the tumor retention of these compounds in tumors is the length of the alkyl chain that determines their hydrophobic properties. Decreasing the chain length from C12 to C7 resulted in little or no tumor accumulation and rapid clearance of the compound in tumor-bearing rats within 24 h of administration. Increasing the chain length had the opposite effect, with the C15 and C18 analogues displaying delayed plasma clearance and enhanced tumor uptake and retention in tumor-bearing rats. Tumor uptake displayed by propanediol analogues NM-412 and NM-413 was accompanied by high levels of liver and abdominal radioactivity 24 h postinjection to tumor-bearing rats. Addition of a 2-*O*-methyl moiety to the propanediol backbone also retarded tumor uptake significantly. A direct comparison between NM-404 and its predecessor, NM-324, in human PC-3 tumor bearing immune-compromised mice revealed a dramatic enhancement in both tumor uptake and total body elimination of NM-404 relative to NM-324. On the basis of imaging and tissue distribution studies in several rodent tumor models, the C18 analogue, NM-404, was chosen for follow-up evaluation in human lung cancer patients. Preliminary results have been extremely promising in that selective uptake and retention of the agent in tumors is accompanied by rapid clearance of background radioactivity from normal tissues, especially those in the abdomen. These results strongly suggest that extension of the human trials to include other cancers is warranted, especially when NM-404 is radiolabeled with iodine-124, a new commercially available positron-emitting isotope. The relatively long physical half-life of 4 days afforded by this isotope appears well-suited to the pharmacodynamic profile of NM-404.

Introduction

In the late 1960s, Snyder and co-workers[1,2] performed a series of experiments designed to evaluate the lipid composition of normal and neoplastic tissues. It was discovered that both animal and human tumor tissue contained much larger quantities of naturally occurring ether lipids relative to corresponding normal tissues. When subsequent studies demonstrated that tumor tissue had less than normal amounts of the enzyme *O*-alkyl glycerol monooxygenase (EC 1.14.16.5, AGMO),[3] it was proposed that differences in the tissue concentration of this ether cleavage enzyme were responsible for the accumulation of ether lipids in tumors. More recent evidence, however, has argued against AGMO deficiency being the sole reason for the elevated ether lipid levels, since certain phospholipid ether analogues that are not substrates for this enzyme also have the capacity to accumulate in tumors.[4] A recent hypothesis that a still unidentified cell surface protein may be involved in the specific incorporation of antitumor lipids into cancer cells has also been advanced.[5]

We have previously described the remarkable capacity of certain radioiodinated phospholipid ether (PLE) analogues (Figure 1) to be selectively retained by a variety of rodent and human tumor cells.[6−14] Moreover, this property made it possible to obtain images of these tumors in rabbits, rats, and mice using γ-camera scintigraphy.

The reason for the retention of PLE and analogues in cancer cells remains unknown. The prevailing hypothesis, however, is that radioiodinated phospholipid ether analogues such as NM-324 (**2**) become trapped in tumor cell membranes because of their inability to be metabolized and eliminated. On the other hand, such lipid molecules are metabolized and cleared by normal tissues, including the liver. Support for this hypothesis was found when lipid extraction of tumors following administration of radioiodinated PLE to tumor-bearing animals showed only the presence of the intact agent, whereas similar analysis of urine and feces revealed only the presence of metabolites.[10]

* Corresponding author. Tel: (608) 262-6376. Fax: (608) 263-4014. E-mail: j.weichert@hosp.wisc.edu.
[†] Department of Pharmacology, University of Michigan Medical School.
[‡] University of Wisconsin Medical School.
[#] Current address: Department of Radiology, E3 Clinical Science Center, 600 Highland Avenue, Madison, WI 53792-3252.
[§] VA Medical Center.
[||] Department of Radiology, University of Michigan Medical School.

10.1021/jm050252g CCC: $33.50 © 2006 American Chemical Society
Published on Web 03/14/2006

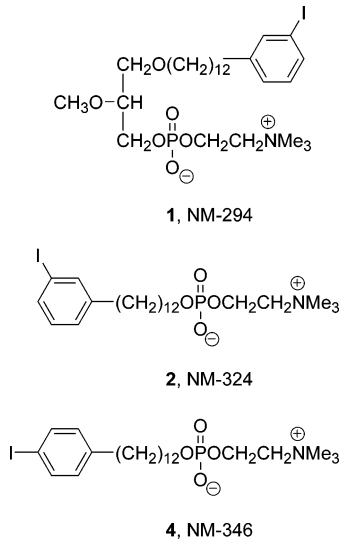

Figure 1.

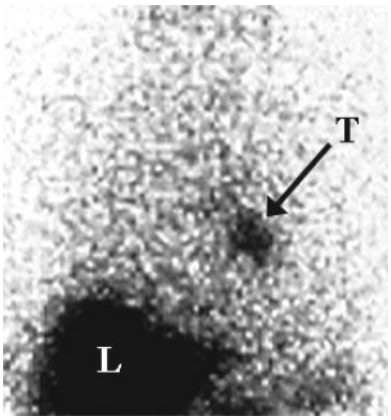

Figure 2. Scintigraphic image obtained in lung cancer patient with ^{131}I-NM-324 6 days after administration (T = lung tumor; L = liver).

Without knowing the precise mechanism for the tumor retention of PLE, the strategy for designing agents with properties superior to NM-324 has been largely empirical. Early work was conducted with meta-iodinated compounds, because it was thought that the iodine would be more metabolically stable in this position. However, synthesis and biological evaluation of para-iodinated PLE analogues demonstrated an equivalent or greater tumor avidity than the corresponding meta-isomers along with minimal in vivo metabolic deiodination.[11,12] One of these compounds, NM-346 (**4**), the para-isomer of NM-324, also displayed significant tumor avidity in the Walker tumor-bearing rat.

As a result of promising rodent studies, a preliminary pharmacokinetic analysis of NM-324 (**2**) was undertaken in cancer patients in order to extend the findings from our animal models into humans.[6] These patient studies demonstrated that NM-324 was taken up and retained by tumors in concentrations sufficient for diagnostic imaging (Figure 2). However, the study results also showed that significant uptake by the liver and clearance by the kidneys caused unacceptable levels of radioactivity to localize in these organs. While these studies served to indicate the relevance of our animal models, they also demonstrated the need to develop agents with superior tumor/liver and tumor/kidney ratios. High tumor uptake observed with NM-324 initiated efforts to make structural modifications in order to determine the structure−activity relationship for

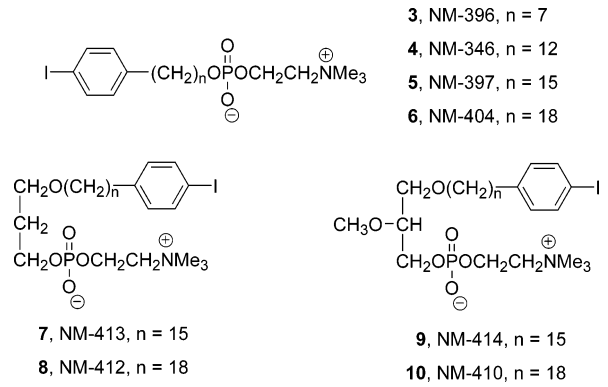

Figure 3.

enhanced tumor retention. In the interest of decreasing liver uptake and increasing plasma half-life, a series of second-generation PLE analogues (**4**−**10**) was synthesized with variations in the alkyl chain length. The alkyl chain modifications made to the phospholipid ether structure are summarized in Figure 3. Accordingly, this paper analyzes the effect of altering the structure of iodinated phospholipid ether analogues in order to determine the resulting influence on (1) tumor retention and (2) uptake in nontarget tissues such as liver and kidney.

Results and Discussion

Chemical Synthesis. In the course of the synthesis of iodinated phospholipid ether analogues, we sought to develop a general synthetic scheme that would allow altering the chain length in the target compounds. Our synthetic approach was based on the copper-catalyzed cross-coupling reaction of Grignard reagents with alkyl tosylates or halides[15] (Schemes 1 and 2). The choice of the building blocks for alkyl chain elongation was dictated by the commercial availability of the starting materials. The synthesis was initiated by the conversion of *p*-iodobenzyl alcohol **11** to *p*-iodobenzyl bromide **12**, as shown in Scheme 1. *p*-Iodobenzyl bromide was further coupled with Grignard reagent derived from THP-protected 11-bromoundecanol **13** in the presence of 0.5−0.7 mol % of Li_2CuCl_4. 12-(*p*-Iodophenyl)dodecanol **17** obtained after deprotection of the first coupling product **16** was used for the synthesis of C12 iodinated phospholipids as described earlier.[12,13] Alcohol **17** also served as a starting material for the synthesis of ω-iodophenyl alkanols with longer chains. For example, coupling of the tosylate **18** with Grignard reagents made from bromides **14** and **15** followed by THP deprotection furnished the C15 (**20**) and C18 (**22**) alcohols, respectively. These alcohols were converted into corresponding alkylphosphocholines **5** (NM-397) and **6** (NM-404) according to published procedures.[12,13] Propanediol phospholipid ethers **7** (NM-413) and **8** (NM-412) were synthesized from 3-benzyloxypropanol **25**, and 2-*O*-methyl-*rac*-glycerol phospholipid ethers **9** (NM-414) and **10** (NM-410) were obtained from 1-*O*-benzyl-2-*O*-methyl-*rac*-glycerol **26**[16] using a sequence of reactions we had previously reported.[12,13] Radiolabeling with iodine-125 was accomplished by an isotope exchange method routinely employed in our laboratory.[17]

Biology. The avidity of PLE analogues to localize in tumors was evaluated in several animal models. The PC-3 model represents a human tumor cell line that was used to determine the target (tumor) to nontarget ratio of NM404 and NM412 in head to head comparison in order to select a candidate for an initial human pharmacokinetic trial in prostate cancer patients. The MatLyLu (Dunning R3327 rat) model, a rat prostate tumor line, was used specifically to screen nine specific analogues prior

Scheme 1[a]

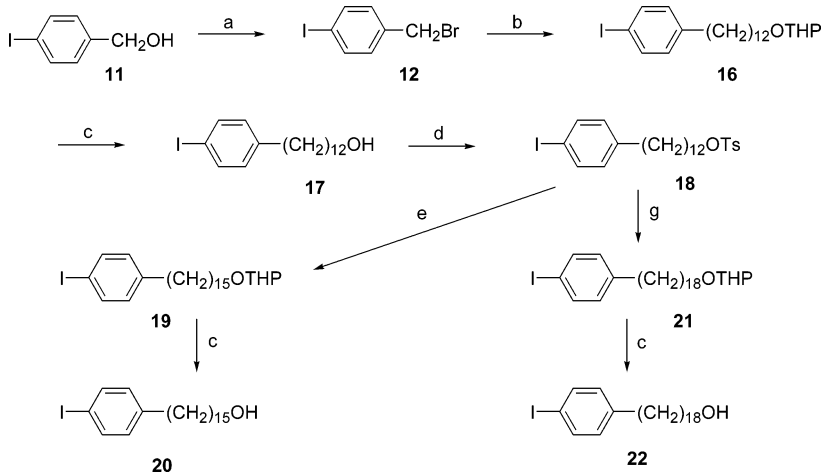

[a] Reagents and conditions: (a) Me_3SiBr, CH_2Cl_2; (b) $BrMg(CH_2)_{11}OTHP$, Li_2CuCl_4 (cat.), THF, −78 to 20 °C; (c) PPTS, EtOH, 40 °C; (d) TsCl, DMAP, CH_2Cl_2; (e) $BrMg(CH_2)_3OTHP$, Li_2CuCl_4 (cat.), THF, −78 to 20 °C; (g) $BrMg(CH_2)_6OTHP$, Li_2CuCl_4 (cat.), THF, −78 to 20 °C.

Scheme 2

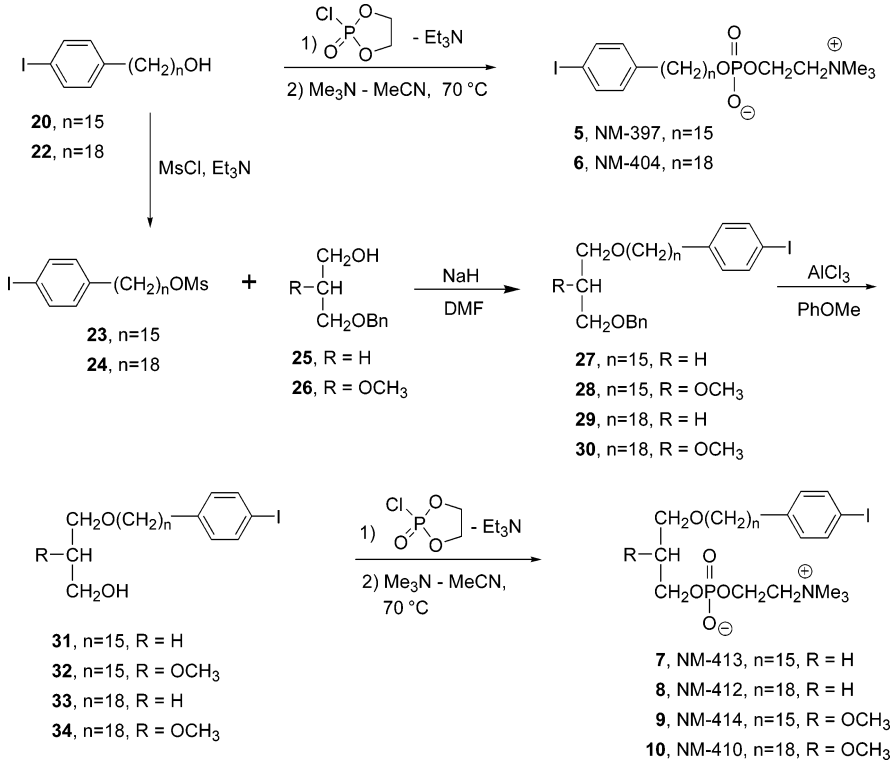

to entering them into control animals for dosimetry and tumor-bearing animals for determining tumor/background ratios. Finally, the Walker-256 carcinosarcoma model was used for quantitative tissue distribution purposes.

To expedite the screening process and minimize the number of tumor-bearing animals utilized in multiple time point tissue distribution studies, new radioiodinated homologues were imaged by γ-camera scintigraphy in the rat Dunning R3337 (MAT LyLu strain) prostate cancer model. Thus, male Copenhagen rats received subcutaneous injection of MAT LyLu cells (1×10^6 cells) in the thigh 10−14 days prior to injection of the radioiodinated PLE analogues (30−40 μCi) in 2% Tween-20 solution. γ-Camera images were obtained at multiple time points including 24 and 48 h postinjection. Homologues (NM-410, NM-413, and NM-414) displaying high hepatic uptake, significant abdominal accumulation, and retention or poor tumor uptake and retention were not submitted to subsequent biodistribution analysis. Tissue distribution of radioactivity in rats bearing Walker-256 carcinosarcoma was assessed at various time intervals following intravenous administration of the radioiodinated chain length homologues. The first group of compounds that was tested included three alkylphosphocholines: a shorter chain analogue with seven carbons, **3** (NM-396), and two analogues with a longer chain length, **5** (NM-397, C15 alkyl chain length) and **6** (NM-404, C18 alkyl chain length).

Initial biodistribution experiments performed with **3** (NM-396, C7 analogue, Table 1) indicated rapid tissue clearance accompanied by significant in vivo deiodination. By 24 h, the amount of radioactivity in the thyroid was 213% injected dose/gram (ID/g), whereas levels of radioactivity in all of the organs surveyed was <0.10% ID/g. As follows from these studies, reducing the number of methylene groups to seven apparently afforded a much more hydrophilic molecule that was rapidly

Table 1. Tissue Distribution over Time of Phospholipid Ether Analogue **3** (NM-396) in Walker 256-Tumor-Bearing Rats after Iv Injection[a]

tissue	6 h ($n = 3$)	24 h ($n = 3$)	48 h ($n = 3$)
adrenal	0.16 ± 0.01	0.04 ± 0.00	0.02 ± 0.00
blood	0.29 ± 0.02	0.03 ± 0.00	0.01 ± 0.00
duodenum	0.20 ± 0.02	0.02 ± 0.00	0.01 ± 0.00
heart	0.11 ± 0.00	0.02 ± 0.00	0.01 ± 0.00
kidney	0.57 ± 0.03	0.09 ± 0.01	0.04 ± 0.00
liver	0.40 ± 0.01	0.06 ± 0.00	0.03 ± 0.00
lung	0.19 ± 0.01	0.04 ± 0.00	0.02 ± 0.00
muscle	0.04 ± 0.01	0.02 ± 0.00	0.01 ± 0.00
ovary	0.17 ± 0.01	0.06 ± 0.00	0.03 ± 0.00
plasma	0.45 ± 0.03	0.05 ± 0.01	0.02 ± 0.00
spleen	0.11 ± 0.01	0.03 ± 0.00	0.02 ± 0.00
thyroid	65.33 ± 18.98	212.96 ± 38.40	71.84 ± 4.59
tumor	0.15 ± 0.01	0.04 ± 0.00	0.03 ± 0.01

[a] Results are expressed as mean % administered dose per gram ±SEM.

Table 2. Tissue Distribution over Time of NM-397 (**5**) in Walker 256-Tumor-Bearing Rats after Iv Injection[a]

tissue	6 h ($n = 3$)	24 h ($n = 4$)	48 h ($n = 3$)	120 h ($n = 3$)
adrenal	0.99 ± 0.07	0.73 ± 0.08	0.49 ± 0.05	0.27 ± 0.01
blood	0.27 ± 0.02	0.16 ± 0.01	0.14 ± 0.01	0.07 ± 0.00
duodenum	0.97 ± 0.15	1.13 ± 0.13	1.38 ± 0.24	0.55 ± 0.11
heart	0.37 ± 0.00	0.31 ± 0.02	0.28 ± 0.02	0.12 ± 0.01
kidney	1.40 ± 0.08	1.14 ± 0.11	0.91 ± 0.04	0.36 ± 0.05
liver	3.08 ± 0.61	1.29 ± 0.10	0.83 ± 0.04	0.51 ± 0.01
lung	1.07 ± 0.30	0.97 ± 0.03	0.81 ± 0.04	0.40 ± 0.02
muscle	0.26 ± 0.15	0.10 ± 0.02	0.08 ± 0.00	0.04 ± 0.00
ovary	0.93 ± 0.07	0.72 ± 0.10	0.41 ± 0.04	0.23 ± 0.01
plasma	1.06 ± 0.04	0.16 ± 0.01	0.15 ± 0.01	0.07 ± 0.01
spleen	1.08 ± 0.03	0.86 ± 0.05	0.70 ± 0.04	0.32 ± 0.02
thyroid	2.27 ± 0.26	11.60 ± 5.40	13.61 ± 3.19	18.13 ± 3.44
tumor	0.72 ± 0.06	1.47 ± 0.10	1.65 ± 0.23	0.87 ± 0.09

[a] Results are expressed as mean % administered dose per gram ±SEM.

excreted by the kidneys. In contrast to compound **4** (NM-346, the C12 analogue), the C7 analogue **3** cleared rapidly from the rat and did not localize in tumor tissue at any of the time points examined.

This observation directed our future efforts to assessing the effect of increasing the length of the aliphatic chain upon tumor uptake and retention. The tissue distribution of the C15 homologue **5** (NM-397) was assessed utilizing the same Walker 256 rat tumor model (Table 2). Radioactivity in the tumor increased with time and peaked at 48 h after administration (1.65 ± 0.23% ID/g) as opposed to most normal tissues, which exhibited their highest levels of radioactivity 6 h after administration. With the exception of thyroid, the tumor had higher radioactivity concentrations at 24, 48, and 120 h than any of the other tissues surveyed. A more rapid washout of radioactivity occurred in the normal tissues as compared to the tumor, presumably due to metabolism and elimination by normal tissues. The accumulation of radioactivity in the thyroid increased throughout the course of the study, suggesting the presence of a low level of in vivo deiodination. Levels of radioactivity in the duodenum were similar to those of tumor, with maximum levels being observed at 48 h after administration (1.38 ± 0.24% ID/g).

Although limited results were obtained with the C12 analogue **4** (NM-346) in this model, results suggest that the tissue distribution profile of the C15 analogue **5** (NM-397) was similar to that observed with the C12 analogue **4** (Table 4) with the exception of a 2-fold increase in tumor uptake at 24 h. The remaining uptake and clearance in other organs and tissues was similar between the two compounds.

The effect of further extending the aliphatic chain to the C18 analogue **6** (NM-404) is displayed in Table 3. The dynamic profile of this compound was similar to that of the C15 analogue **5** (NM-397), as levels of radioactivity peaked in the tumor 48 h after administration (1.14 ±0.01% ID/g), albeit at slightly lower levels. Quantities of radioactivity detected in liver, kidney, and duodenum were significantly lower following administration of the C18 compound **6** as compared to the same organs in the C15 analogue **5** studies. In addition, the C18 analogue **6** was retained in the circulation to a much greater extent than the other chain length homologues surveyed. For example, at 120 h, blood levels for **6** were 0.6 ± 0.1% ID/g as compared to levels of 0.07 ±0.00% ID/g for the C15 (**5**) analogue. Total radioactivity levels in the thyroid were relatively low in both **5** and **6** when the extremely small mass of the gland is considered. Table 4 contains a comparative summary of the data obtained for the biodistribution of the alkyl chain length homologues.

To examine the transport properties of PLE analogues, plasma was isolated from Walker 256-tumor-bearing rats 7 days after administration of iodine-125-labeled **6**. The distribution of radioactivity in the plasma compartment of a rat receiving **6** (NM-404) is shown in Table 5. PAGE analysis revealed that most of the circulating radioactivity (88%) was associated with the albumin fraction following administration of the C18 analogue **6**. This finding is similar to results reported by Eibl,[18] who studied binding of phospholipid ether prototype ET-18-OCH_3 with serum proteins and found that the majority of the ether lipid (71%) was bound to albumin and about 6% to HDL.

Comparative Imaging Studies. γ-Camera scintigraphy images shown in Figure 4 directly compare the tumor uptake and body clearance of second-generation analogue ^{125}I-NM-404 (**6**) versus its shorter chain, first-generation predecessor ^{125}I-NM-324 (**2**) at 1, 2, and 4 days postadministration in immune-compromised SCID mice bearing human PC-3 prostate tumor xenografts. Qualitative scintigraphic comparison of these two PLE analogues demonstrated a striking difference in tumor

Table 3. Tissue Distribution over Time of NM-404 (**6**) in Walker 256-Tumor-Bearing Rats after Iv Injection[a]

tissue	6 h ($n = 3$)	24 h ($n = 3$)	48 h ($n = 3$)	120 h ($n = 2$)	168 h ($n = 1$)
adrenal	0.87 ± 0.08	0.85 ± 0.04	0.92 ± 0.06	0.60 ± 0.01	0.48
blood	1.28 ± 0.02	0.96 ± 0.00	0.64 ± 0.07	0.55 ± 0.10	0.61
duodenum	0.85 ± 0.08	0.69 ± 0.05	0.68 ± 0.04	0.42 ± 0.02	0.45
heart	0.53 ± 0.02	0.38 ± 0.02	0.32 ± 0.02	0.25 ± 0.02	0.28
kidney	0.87 ± 0.06	0.65 ± 0.00	0.59 ± 0.04	0.42 ± 0.02	0.41
liver	1.05 ± 0.11	0.55 ± 0.04	0.59 ± 0.05	0.34 ± 0.04	0.32
lung	1.14 ± 0.10	0.88 ± 0.06	0.76 ± 0.07	0.56 ± 0.00	0.62
muscle	0.18 ± 0.01	0.13 ± 0.01	0.10 ± 0.01	0.07 ± 0.01	0.16
ovary	0.98 ± 0.09	0.90 ± 0.03	0.68 ± 0.08	0.47 ± 0.05	0.46
plasma	1.96 ± 0.05	1.47 ± 0.03	0.95 ± 0.11	0.79 ± 0.10	0.83
spleen	0.84 ± 0.07	0.59 ± 0.03	0.65 ± 0.06	0.35 ± 0.03	0.31
thyroid	10.73 ± 0.67	13.40 ± 0.46	11.46 ± 0.86	6.08 ± 0.44	4.60
tumor	0.55 ± 0.04	0.98 ± 0.07	1.14 ± 0.01	0.89 ± 0.08	0.81

[a] Results are expressed as mean % administered dose per gram ±SEM.

Table 4. Biodistribution over Time of Phospholipid Ether Analogues in Walker 256-Tumor-Bearing Rats 24 and 48 h after Iv Injection[a]

	C7 analogue ±NM-396)		C12 analogue ±NM-346)		C15 analogue ±NM-397)		C18 analogue ±NM-404)	
tissue	24 h ($n = 3$)	48 h ($n = 3$)	24 h ($n = 3$)	48 h ($n = 3$)	24 h ($n = 3$)	48 h ($n = 3$)	24 h ($n = 4$)	48 h ($n = 3$)
adrenal	0.04 ± 0.00	0.02 ± 0.00	0.33 ± 0.01	0.29 ± 0.01	0.73 ± 0.08	0.49 ± 0.05	0.85 ± 0.04	0.92 ± 0.06
blood	0.03 ± 0.00	0.01 ± 0.00	0.29 ± 0.02	0.27 ± 0.03	0.16 ± 0.01	0.14 ± 0.01	0.96 ± 0.00	0.64 ± 0.07
duodenum	0.02 ± 0.00	0.01 ± 0.00	0.44 ± 0.16	0.77 ± 0.06	1.13 ± 0.13	1.38 ± 0.24	0.69 ± 0.05	0.68 ± 0.04
heart	0.02 ± 0.01	0.01 ± 0.00	0.21 ± 0.02	0.19 ± 0.01	0.31 ± 0.02	0.28 ± 0.02	0.38 ± 0.02	0.32 ± 0.02
kidney	0.09 ± 0.01	0.04 ± 0.00	0.41 ± 0.04	0.34 ± 0.08	1.14 ± 0.11	0.91 ± 0.04	0.65 ± 0.00	0.59 ± 0.04
liver	0.06 ± 0.00	0.03 ± 0.00	1.74 ± 0.17	1.37 ± 0.01	1.29 ± 0.10	0.83 ± 0.04	0.55 ± 0.04	0.59 ± 0.05
lung	0.04 ± 0.00	0.02 ± 0.00	0.63 ± 0.03	0.53 ± 0.01	0.97 ± 0.03	0.81 ± 0.04	0.88 ± 0.06	0.76 ± 0.07
muscle	0.02 ± 0.00	0.01 ± 0.00	0.06 ± 0.01	0.06 ± 0.01	0.10 ± 0.02	0.08 ± 0.00	0.13 ± 0.01	0.10 ± 0.01
ovary	0.06 ± 0.00	0.03 ± 0.00	0.37 ± 0.03	0.33 ± 0.01	0.72 ± 0.10	0.41 ± 0.04	0.90 ± 0.03	0.68 ± 0.08
plasma	0.05 ± 0.01	0.02 ± 0.00	0.39 ± 0.05	0.39 ± 0.05	0.16 ± 0.01	0.15 ± 0.01	1.47 ± 0.03	0.95 ± 0.11
spleen	0.03 ± 0.00	0.02 ± 0.00	0.42 ± 0.01	0.32 ± 0.01	0.86 ± 0.05	0.70 ± 0.04	0.59 ± 0.03	0.65 ± 0.06
thyroid	212.96 ± 38.40	71.84 ± 4.58	90.8 ± 14.8	85.2 ± 7.4	11.60 ± 5.4	13.61 ± 3.19	13.40 ± 0.46	11.46 ± 0.86
tumor	0.04 ± 0.00	0.03 ± 0.01	2.05 ± 0.32	1.84 ± 0.09	1.47 ± 0.10	1.65 ± 0.23	0.98 ± 0.07	1.14 ± 0.01

[a] Results are expressed as mean % administered dose per gram ±SEM.

Table 5. Distribution of Radioactivity in the Plasma Samples from Walker-256-Tumor-Bearing Rats ($n = 3$, ±SEM) Receiving 6 (NM-404) Collected 168 Hours after Iv Administration, As Determined by Polyacrylamide Gel Electrophesis (PAGE)

stacking gel	1.17 ± 0.08
LDL	2.84 ± 1.37
HDL	7.24 ± 1.03
albumin	87.81 ± 0.52
below albumin	0.94 ± 0.01

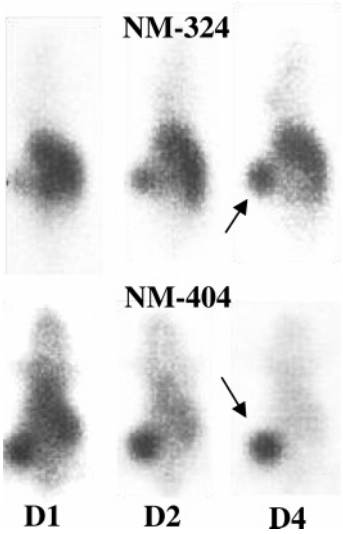

Figure 4. Scintigraphic comparison of NM-324 (top panel) and NM-404 (bottom panel) at 1, 2, and 4 days postinjection in a SCID mouse with human prostate PC-3 tumor (arrow) implanted in the flank. Liver and abdominal background radioactivities are much lower with NM-404 relative to NM-324.

uptake and overall body clearance. The longer chain agent, NM-404, displays rapid tumor uptake and prolonged retention accompanied by rapid whole body elimination of radioactivity, whereas tumor uptake and body clearance are substantially delayed with NM-324, even at 4 days following administration. Significant tumor uptake and retention of C18 analogue NM-404 accompanied by rapid whole body elimination clearly defined the superior imaging properties of NM-404 in this model.

Extensive quantitative tissue distribution results obtained at 1, 3, 5, and 8 days following administration of radioiodinated NM-404 in this model (Table 6) indicated rapid elimination of radioactivity from all normal tissues over the 8-day evaluation period. Tumor uptake, however, continued to increase up until day 5, when it reached 18% ID/g of tumor. Tumor to background tissue ratios steadily increased over the course of the experiment, due to prolonged retention in tumors coupled with a steady elimination from normal tissues. Tumor to background tissue ratios exceeded 4, 6.8, 23, and 9 in blood, liver, muscle, and prostate, respectively, 3 days after injection and continued to improve at 5 and 8 days. Again, although thyroid levels ranged from 26 to 54% injected dose per gram of tissue, these levels are actually quite low and represent an extremely small percentage of the injected dose when the exceedingly small mass of the organ is considered, and the data are presented on a percent administered dose per organ basis.

Kötting et al have investigated the effects of alkyl chain length on the biodistribution of three alkyl phosphocholine (APC) analogues.[19] The Kötting study differed from our experiments in that (1) compounds were orally administered at concentrations thought to be cytotoxic to tumor and (2) the C22 compound contained a double bond in the alkyl chain. Therefore, direct comparisons with the work described herein cannot be made due to large dose differences and the unknown bioavailability of the oral agents. In the Kötting study, C16, C18, and C22 analogues were administered orally to rats bearing a methylnitrosourea-induced mammary carcinoma in daily doses of 50−120 μmol/kg. As alkyl chain length increased, the observed levels of compound in kidney, liver, and lung decreased. In contrast to our tracer results obtained with the radioiodinated PLE analogues, Kötting and co-workers found that levels of APC in blood decreased with increasing chain length, while tumor levels increased with increasing chain length.[19] It would be expected that oral administration would result in a substantial amount of degradation of the ether lipids in the GI tract prior to absorption.

Tumors were readily visualized with the C12 (**4**), C15 (**5**), and C18 (**6**) alkyl phosphocholine homologues via γ-camera scintigraphy at both 24 and 48 h after injection. Rat imaging results obtained with C15 (**7**, NM-413) and C18 (**8**, NM-412) propanediol analogues, on the other hand, displayed tumor uptake accompanied by high liver and abdominal radioactivity levels (Figure 5). Imaging results obtained with C15 (**9**, NM-414) and C18 (**10**, NM-410) 2-*O*-Me glycerol analogues in the MAT LyLu prostate model indicated high radioactivity levels in the liver and abdomen with little to no uptake of the agent into tumors (Figure 5). The differences in the clearance and quantity of radioactivity from nontarget tissues including the liver and intestinal tract will have significant impact upon the application of radioiodinated phospholipid ether analogues as imaging agents in humans. Nontarget tissue uptake can decrease the efficacy of radiodiagnostic imaging by creating high background activity or by causing excessive exposure of

Table 6. Biodistribution over Time of ^{125}I-NM-404 in Male SCID Mice Bearing PC-3 Prostate Cancer Xenografts[a]

	day 1		day 3		day 5		day 8	
tissue	% dose/g	tumor/ bkg[b]	% dose/g	tumor/ bkg	% dose/g	tumor/ bkg	% dose/g	tumor/ bkg
adrenal	7.83 ± 0.78	1.2	4.65 ± 0.40	2.8	4.76 ± 0.51	3.8	3.00 ± 0.51	5.0
blood	5.74 ± 0.20	1.6	3.10 ± 0.13	4.2	3.08 ± 0.09	5.9	2.17 ± 0.09	6.9
fat	2.39 ± 0.33	3.8	1.26 ± 0.21	10.5	1.11 ± 0.09	16.3	0.87 ± 0.09	17.2
heart	2.81 ± 0.10	3.3	1.45 ± 0.04	9.1	1.38 ± 0.06	13.1	0.97 ± 0.06	15.4
kidney	4.22 ± 0.14	2.2	2.15 ± 0.11	6.1	2.28 ± 0.09	7.9	1.46 ± 0.09	10.3
liver	3.69 ± 0.22	2.5	1.93 ± 0.10	6.8	1.63 ± 0.06	11.1	1.02 ± 0.06	14.7
lung	5.36 ± 0.33	1.7	2.60 ± 0.20	5.1	2.27 ± 0.09	8.0	1.54 ± 0.09	9.7
muscle	0.80 ± 0.03	11.5	0.57 ± 0.04	23.0	0.49 ± 0.03	37.0	0.40 ± 0.03	37.3
plasma	9.93 ± 0.53	0.9	5.27 ± 0.16	2.5	5.41 ± 0.14	3.3	3.98 ± 0.14	3.8
prostate	2.61 ± 0.15	3.5	1.40 ± 0.27	9.4	1.96 ± 0.25	9.2	1.41 ± 0.25	10.6
spleen	4.99 ± 0.37	1.8	2.24 ± 0.12	5.9	1.99 ± 0.10	9.1	1.36 ± 0.10	11.0
thyroid	42.68 ± 10.72	0.2	54.53 ± 12.54	0.2	26.48 ± 4.00	0.7	33.90 ± 11.02	0.4
tumor	9.14 ± 0.69	1.0	13.14 ± 0.40	1.0	18.06 ± 0.81	1.0	14.96 ± 0.63	1.0

[a] Results are expressed as mean % administered dose per gram ±SEM (n = 4 for each time point). [b] Tumor to background tissue ratio based on % administered dose per gram basis.

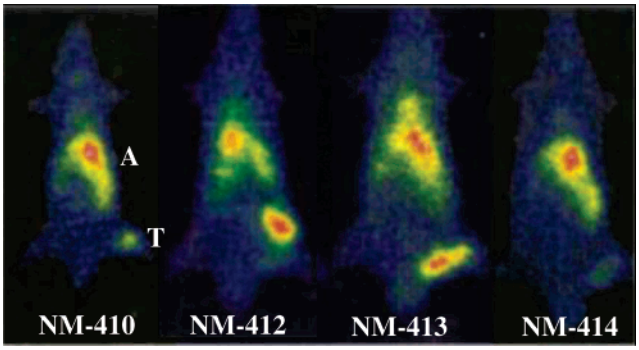

Figure 5. Representative γ-camera scans of the propanediol analogues **7** (NM-413, C15), **8** (NM-412, C18), **9** (NM-414, C15), and **10** (NM-410, C18) in MAT-LyLu tumor-bearing rats 24 h after iv administration. The presence of the 2-*O*-methyl moiety in **9** and **10** retards tumor uptake significantly in this series. Rats were injected with I-125-labeled PLE (35−50 μCi) and scanned for 20 min (A = abdominal activity associated with liver, kidney, and GI tract. T = tumor).

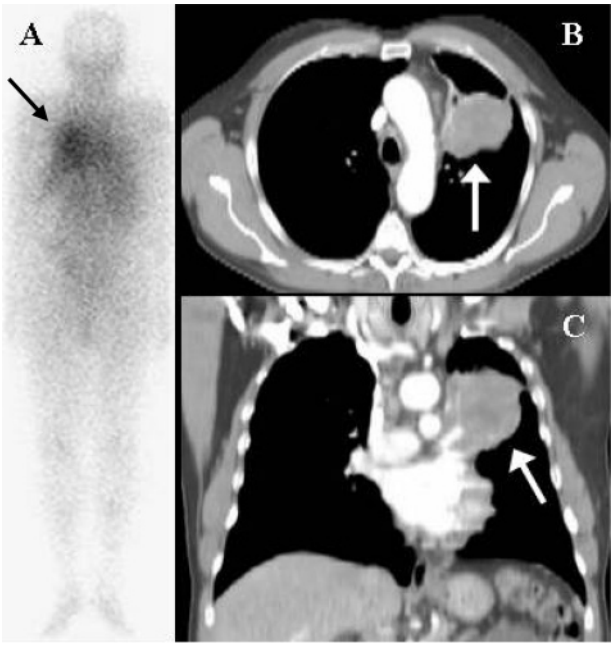

Figure 6. Posterior whole-body planar nuclear medicine image (A) 4 days after iv administration of ^{131}I-NM-404 (0.8 mCi) to a patient with non-small-cell lung cancer (6 cm dia., arrow). Lung tumor is easily detected in corresponding axial (B) and coronal (C) computed tomography (CT) scans.

radiosensitive tissues to the injected radioactivity. A preliminary clinical trial with **2** (NM-324, the *m*-iodo isomer of NM-346) in cancer patients, while affording excellent tumor uptake, was limited by the radiation dosimetry associated with accumulation in nontarget tissues including liver, kidneys, and bladder (Figure 2).[6]

Our strategy was to examine the alkyl portion of phospholipid ether analogue structure and determine its role in tumor localization and retention. Qualitative rat whole body screening scans acquired in MAT-LyLu tumor bearing rats with radioiodinated PLE analogues with longer chain lengths revealed sufficient tumor uptake to permit detection. However, follow-up tissue distribution studies have shown that sequential increases in the chain length from C12 to C15 to C18, resulted in a rapid decline in the amount of radioactivity detected in the nontarget organs. This substantial decrease in nontarget tissue activity was accompanied by a relatively small reduction in the levels of radioactivity present in the tumor. In addition, the C18 analogue **6** (NM-404) displayed a propensity to remain in the circulation much longer than the C12 (**4**) and C15 (**5**) analogues. A longer plasma half-life may be expected to result in additional opportunities for uptake of the C18 compound **6** by the tumor as it continually circulated through the vasculature. This extended plasma half-life may be a result of strong binding of the probe to albumin (Table 5). Uptake and transport of radiolabeled PLE by plasma components may also be an important factor related to the tumor retention of these compounds. Certainly, increase of the chain length from C7 to C18, results in an increase in the lipophilicity of the PLE analogues. Greater lipophilicity may increase the affinity of these compounds for the cell membrane and may alter their binding to plasma components. Uptake and transport in the circulation by endogenous lipoproteins such as LDL and HDL may also impact the biological distribution into the tumor.

In preparation for human clinical trials, unlabeled NM404 was subjected to independent (University of Buffalo Toxicology Research Center) acute toxicity evaluation at 1200 times the anticipated imaging mass dose in rats and rabbits. The agent was well-tolerated and no acute toxicities were found at this dose level. Due to its selective tumor uptake and retention properties in a variety of rodent tumor models and subsequent excellent safety profile in rats and rabbits, NM-404 was selected to undergo initial human pharmacokinetic evaluation in non-small-cell lung cancer (NSCLC) patients. Patients underwent planar γ-camera scintigraphy after receiving an injection of ^{131}I-NM-404 (<1 mCi). Preliminary human results (n = 3)

demonstrated tumor uptake and prolonged retention in the primary lung tumors (Figure 6). Relative to the high liver uptake values observed with its predecessor, NM-324, however, liver and abdominal radioactivity levels were much lower with NM-404, suggesting the feasibility of evaluating this agent in other abdominal tumors, including those associated with the colon, prostate, and pancreas.

Conclusions

In summary, the rationale behind the design of new iodinated PLE analogues described in this paper was exploited in an effort to evaluate the effect of chain length and other structural modifications in the hydrophobic part of the phospholipid molecule on tumor uptake and retention. Decreasing the chain length from C12 to C7 resulted in little or no tumor accumulation and rapid clearance of the compound in tumor-bearing rats by 24 h after administration. Increasing the chain length had the opposite effect, with the C15 and C18 analogues displaying delayed plasma clearance and enhanced tumor uptake and retention in tumor-bearing rats. Tumor uptake displayed by propanediol analogues **7** and **8** was accompanied by fairly high levels of liver and abdominal radioactivity 24 h postinjection to tumor-bearing rats. Addition of a 2-*O*-methyl moiety in **9** and **10** retarded tumor uptake significantly. A direct comparison between NM-404 and its predecessor, NM-324, in human PC-3 bearing immune-compromised mice revealed a dramatic enhancement in both tumor uptake and total body elimination of NM-404 relative to NM-324. NM-404 afforded superior imaging properties to the other analogues examined in several animal models, thus warranting further evaluation of this second-generation PLE analogue in human lung cancer patients. Preliminary clinical results in humans indicated desired tumor uptake and retention properties similar to those seen previously in animal models. In contrast to its shorter chain predecessor NM-324, however, NM-404 displayed significantly lower liver, kidney, and abdominal background radioactivity levels, which in addition to providing promise for lung tumor imaging, suggests further evaluation of this agent in human colorectal, pancreatic, and prostate cancer patients is warranted. Moreover, a lack of urinary bladder radioactivity suggests little renal clearance of the agent or its metabolites over the time points examined. This represents a significant advantage over ^{18}F-fluorodeoxyglucose (FDG), a PET agent used routinely for tumor imaging today, which undergoes significant renal elimination, thus prohibiting imaging in the area of the prostate.

Because the tumor-targeting strategy of PLE analogues appears to involve selective tumor retention over time, relatively short-lived nuclides such as ^{18}F or even ^{99m}Tc are not practical for labeling NM-404 at the current time. Given the preliminary success of ^{131}I-NM-404 in our current lung cancer imaging trial, it is now imperative to radiolabel NM-404 with iodine-124, a relatively new positron-emitting isotope with a 4.2-day half-life, and to evaluate its tumor detection efficacy by PET. It has been reported that PET imaging with ^{124}I affords over 40 times the sensitivity of planar ^{131}I-γ-imaging.[20] PET, unlike traditional γ-camera imaging, also offers significant resolution enhancement and three-dimensional imaging capabilities, as well as superior quantitation properties[21] relative to planar scintigraphic imaging. The long, 4-day physical half-life of this PET isotope is well-suited to the tumor uptake and retention kinetics of NM-404 and we are in the process of extending our imaging studies with NM-404 to include PET.

Experimental Section

Chemistry. All chemicals were purchased from Aldrich Chemical Co. (Milwaukee, WI). 1-*O*-Benzyl-2-*O*-methyl-*rac*-glycerol **26** was synthesized as described previously.[16] Thin-layer chromatography was performed using DC-Alufolien Kieselgel 60 F_{254} plates (E. Merck, Darmstadt, Germany). Visualization was achieved by UV light and/or charring after spraying with 5% H_2SO_4 in ethanol. For flash chromatography, silica gel 32−63 μm from Fisher Scientific (Hanover Park, IL) was used. Melting points were taken in glass capillary tubes on a Melt-Temp apparatus and are uncorrected. NMR data were collected on Bruker AM-360 or Varian Unity Inova 400 and 500 spectrometers. Chemical shifts are reported in parts per million (ppm) relative to tetramethylsilane (TMS), and spin multiplicities are given as s (singlet), d (doublet), t (triplet), q (quartet), m (multiplet), or br m (broad multiplet). Elemental analyses were performed by the analytical laboratory at the University of Michigan Department of Chemistry. The elemental analyses of the compounds agreed to within ±0.4% of the calculated value. High-resolution mass spectra were obtained on an IonSpec 7 T HiResMALDI FT-mass spectrometer at the Analytical Instrumentation Center of UW School of Pharmacy.

***p*-Iodobenzyl Bromide (12).** Bromotrimethylsilane (2.5 mL, 19.28 mmol) was slowly added with stirring to a solution of *p*-iodobenzyl alcohol **11** (3 g, 12.82 mmol) in anhydrous dichloromethane (15 mL). The mixture was stirred at room temperature for 12 h, quenched with water, and extracted with ethyl acetate. The extract was washed successively with water, $Na_2S_2O_3$ solution, and water and dried over Na_2SO_4. Evaporation of solvent yielded a solid which was crystallized from methanol to give white crystals. Mp: 77−78.5 °C. Yield: 3.207 g (84%). ^{1}H NMR (400 MHz, $CDCl_3$): 7.67 and 7.13 (2 dt, 2H each, IC_6H_4), 4.42 (s, 2H, CH_2). ^{13}C NMR (100 MHz, $CDCl_3$): 137.95, 137.41, 130.82, 94.12, 32.45. Anal. (C_7H_6BrI) C, H.

Tetrahydro-2-(11-bromoundecyloxy)-2*H*-pyran (13). A solution of 11-bromoundecanol (6 g, 24 mmol) and dihydropyran (3.3 mL, 36 mmol) in methylene chloride (20 mL) containing pyridinium *p*-toluenesulfonate (600 mg, 2.4 mmol) was stirred at room temperature for 5 h. The solution was diluted with hexane, washed with water, and dried over Na_2SO_4. Flash chromatography in hexanes−ether (150:5) afforded the product (7.93 g, 99%) as a clear oil. ^{1}H NMR (500 MHz, $CDCl_3$): 4.57 (dd, 1H, anomeric 2-H of THP), 3.90−3.84 (m, 1H, 6-H_{eq} of THP), 3.73 (dt, 1H, CH_AH$_B$-OTHP), 3.54−3.47 (m, 1H, 6-H_{ax} of THP), 3.40 (t, 2H, CH_2Br), 3.38 (dt, 1H, CH$_A$$H_B$OTHP), 1.85 (quintet, 2H, BrCH$_2$CH_2), 1.87−1.79 (m, 1H, 4-H_{eq} of THP), 1.74−1.68 (m, 1H, 3-H_{eq} of THP), 1.62−1.48 (m, 6H, THPOCH$_2$CH_2, 3-H_{ax}, 4-H_{ax}, 5-H_{eq} and 5-H_{ax} of THP), 1.45−1.38 (m, 2H, BrCH$_2$CH$_2$CH_2), 1.38−1.26 (m, 12H, $(CH_2)_6$). ^{13}C NMR (100 MHz, $CDCl_3$): 98.81, 67.64, 62.31, 33.97, 32.80, 30.76, 29.72, 29.49, 29.43, 29.42, 29.37, 28.72, 28.14, 26.20, 25.49, 19.68. Anal. ($C_{16}H_{31}BrO_2$) C, H.

Tetrahydro-2-(3-bromopropyloxy)-2*H*-pyran (14). Following the procedure described for the preparation of **13**, the title compound was obtained from 3-bromopropanol (1 g, 7.2 mmol) in 98% yield as a clear oil. ^{1}H NMR (360 MHz, $CDCl_3$): 4.62−4.59 (m, 1H, anomeric 2-H of THP), 3.90−3.83 (m, 1H, 6-H_{eq} of THP), 3.88 (dt, 1H, CH_AH$_B$OTHP), 3.56−3.48 (m, 1H, 6-H_{ax} of THP), 3.54 (t, 2H, $BrCH_2$), 3.52 (dt, 1H, CH$_A$$H_B$OTHP), 2.14 (quintet, 2H, BrCH$_2$CH_2), 1.84−1.66 (m, 2H, THP), 1.64−1.49 (m, 6H, 4H, THP). Anal. ($C_8H_{15}BrO_2$) C, H.

Tetrahydro-2-(6-bromohexadecyloxy)-2*H*-pyran (15). This compound was prepared from 6-bromohexanol (1.38 g, 7.62 mmol) in 92% yield (clear oil) according to the general procedure described for **13**. ^{1}H NMR (400 MHz, $CDCl_3$): 4.57 (dd, 1H, anomeric 2-H of THP), 3.90−3.83 (m, 1H, 6-H_{eq} of THP), 3.74 (dt, 1H, CH_AH$_B$-OTHP), 3.53−3.47 (m, 1H, 6-H_{ax} of THP), 3.41 (t, 2H, CH_2Br), 3.39 (dt, 1H, CH$_A$$H_B$OTHP), 1.87 (quintet, 2H, BrCH$C H_2$), 1.88−1.67 (m, 2H, THP), 1.66−1.36 (m, 10H, $(CH_2)_3CH_2$OTHP and 4H of THP). ^{13}C NMR (100 MHz, $CDCl_3$): 98.87, 67.37, 62.35, 33.84, 32.72, 30.74, 29.53, 27.97, 25.46, 25.44, 19.67. Anal. ($C_{11}H_{21}BrO_2$) C, H.

Tetrahydro-2-[12-(*p*-iodophenyl)dodecyloxy]-2*H*-pyran (16). Magnesium powder (300 mg, 12.5 mmol) was suspended in THF (2.5 mL), and dibromoethane (0.05 mL) was added for activation. After 10 min, the THF solution was withdrawn by syringe and replaced with 2 mL of fresh THF. A solution of the bromide **13** (3.1 g, 9.25 mmol) in THF (12 mL) was added dropwise over 1 h at room temperature. Then, a solution of Grignard reagent was transferred into a round-bottom flask via cannula and cooled to −78 °C. A solution of Li_2CuCl_4 in THF (0.4 mL of 0.12 mmol/mL solution, 0.048 mmol) was added to the Grignard reagent with stirring followed by a solution of *p*-iodobenzyl bromide **12** (2.45 g, 8.25 mmol) in THF (15 mL). The reaction mixture was allowed to warm to room temperature during 5 h followed by continuous stirring for an additional 12 h. The reaction mixture was quenched with ammonium chloride solution and extracted with ethyl acetate. The extract was washed with water and dried over Na_2SO_4. The solvent was removed in vacuo and the residue was chromatographed on silica gel, first eluting with hexane−chloroform (8:2) and then with hexane−ether (150:3) to give a clear oil (2.16 g, 55%). ^{1}H NMR (500 MHz, $CDCl_3$): 7.58 and 6.92 (2 dt, 2H each, IC_6H_4), 4.57 (dd, 1H, anomeric 2-H of THP), 3.90−3.84 (m, 1H, 6-H_{eq} of THP), 3.73 (dt, 1H, CH_AH$_B$OTHP), 3.52−3.47 (m, 1H, 6-H_{ax} of THP), 3.38 (dt, 1H, CH$_A$$H_B$OTHP), 2.53 (t, 2H, Ar$CH_2$), 1.88−1.79 (m, 1H, 4-$H_{eq}$ of THP), 1.75−1.68 (m, 1H, 3-H_{eq} of THP), 1.62−1.48 (m, 8H, ArCH$_2$CH_2, THPOCH$_2$CH_2, 3-H_{ax}, 4-H_{ax}, 5-H_{eq}, 5-H_{ax} of THP), 1.38−1.22 (m, 16H, $(CH_2)_8$). ^{13}C NMR (100 MHz, $CDCl_3$): 142.52, 137.20, 130.54, 98.84, 90.46, 67.68, 62.34, 35.42, 31.27, 30.79, 29.75, 29.59, 29.56 (2C), 29.52, 29.47, 29.43, 29.17, 26.23, 25.50, 19.70. HRMS: calculated for $C_{23}H_{37}IO_2Na$ (M^+ + Na) 495.1736, found 495.1744. Anal. ($C_{23}H_{37}IO_2$) C, H.

12-(*p*-Iodophenyl)dodecanol (17). A solution of THP ether **16** (4.068 g, 8.62 mmol) and pyridinium *p*-toluenesulfonate (216 mg, 0.86 mmol) in ethanol (20 mL) was stirred at 50 °C for 3 h until TLC showed no starting material. The reaction mixture was diluted with water, extracted with ethyl acetate, washed with water, and dried over Na_2SO_4, and the solvent was evaporated. Silica gel chromatography of the residue in hexane−ethyl acetate (85:15) gave the product (3.01 g, 90%) as a white solid. In cases when contamination by the aliphatic alcohol derived from Grignard reagent was revealed by NMR, the product was crystallized from acetonitrile at 15 °C (for alcohols **20** and **22** at room temperature). Mp: 61.5−63 °C. ^{1}H NMR (400 MHz, $CDCl_3$): 7.58 and 6.92 (2 dt, 2H each, IC_6H_4), 3.64 (q, 2H, CH_2OH), 2.54 (t, 2H, ArCH_2), 1.62−1.50 (m, 4H, ArCH$_2$CH_2 and CH_2CH$_2$OH), 1.40−1.22 (m, 16H, $(CH_2)_8$), 1.21 (t, 1H, OH). ^{13}C NMR (100 MHz, $CDCl_3$): 142.55, 137.24, 130.56, 90.49, 63.11, 35.45, 32.82, 31.29, 29.61, 29.59, 29.56, 29.54, 29.45, 29.43, 29.18, 25.74. Anal. ($C_{18}H_{29}IO$) C, H.

12-(*p*-Iodophenyl)dodecyl Tosylate (18). A solution of 12-(*p*-iodophenyl)dodecanol **17** (2.01 g, 5.18 mmol), tosyl chloride (1.09 g, 5.7 mmol), and *N*,*N*-(dimethylamino)pyridine (0.72 g, 5.9 mmol) in dichloromethane (15 mL) was stirred for 6 h. The clear reaction mixture was diluted with 10 mL of hexane and carefully poured directly onto the top of a silica gel column. The column was eluted with hexane−chloroform (1:1) and then with chloroform to give the tosylate **18** (2.69 g, 96%) as a white solid. Mp: 42−43 °C. ^{1}H NMR (400 MHz, $CDCl_3$): 7.58 and 6.92 (2 dt, 2H each, IC_6H_4), 7.79 and 7.34 (2 dt, 2H each, $CH_3C_6H_4SO_3$), 4.02 (t, 2H, CH_2-OTs), 2.53 (t, 2H, ArCH_2), 2.45 (s, 3H, CH_3C$_6$H$_4$SO$_3$), 1.66−1.52 (m, 4H, ArCH$_2$CH_2 and CH_2CH$_2$OTs), 1.32−1.18 (m, 16H, $(CH_2)_8$). ^{13}C NMR (100 MHz, $CDCl_3$): 144.57, 142.50, 137.21, 133.28, 130.54, 129.77, 127.86, 90.47, 70.68, 35.42, 31.25, 29.53, 29.49, 29.44, 29.41, 29.34, 29.15, 28.90, 28.81, 25.31, 21.62. Anal. ($C_{25}H_{35}IO_3S$) C, H.

Tetrahydro-2-[18-(*p*-iodopheny)octadecyloxy]-2*H*-pyran (21). Magnesium powder (370 mg, 15.4 mmol) in THF (2.5 mL) was activated by addition of 1,2-dibromoethane (0.03 mL) and stirring for 10 min. After the reaction with dibromoethane had ceased, the solution was removed via syringe and replaced with fresh THF (5 mL). This procedure was followed by the addition of bromide **15** (1.373 g, 5.18 mmol) in THF (10 mL) over 0.5 h at room temperature. When all the halide had been added, stirring was continued for an additional 15 min, whereupon a small aliquot was hydrolyzed and analyzed by TLC in hexanes−ether (150:6), which revealed no presence of starting bromide. The Grignard reagent was transferred to a round-bottom flask and cooled to −78 °C. The organometallic reagent was stirred for 10 min at this temperature before a solution of Li_2CuCl_4 in THF (0.5 mL of 0.077 mmol/mL solution, 0.0385 mmol) was added followed by 12-(*p*-iodophenyl)dodecyl tosylate **18** (2.69 g, 4.96 mmol) dissolved in THF (10 mL). The reaction mixture was allowed to gradually warm to room temperature for 3 h and was kept at this temperature for an additional 12 h before a saturated ammonium chloride solution was added to quench the reaction. The mixture was extracted with hexane, washed with water, and dried over Na_2SO_4. The solvent was removed in a vacuum, and silica gel chromatography with hexane−ether (150:3) gave the product (1.77 g, 64%) as a white wax. Mp: 26−27 °C. ^{1}H NMR (360 MHz, $CDCl_3$): 7.58 and 6.92 (2 dt, 2H each, IC_6H_4), 4.59−4.57 (m, 1H, anomeric 2-H of THP), 3.91−3.84 (m, 1H, 6-H_{eq} of THP), 3.73 (dt, 1H, CH_AH$_B$OTHP), 3.54−3.46 (m, 1H, 6-H_{ax} of THP), 3.38 (dt, 1H, CH$_A$$H_B$OTHP), 2.55 (t, 2H, Ar$CH_2$), 1.82−1.67 (m, 2H, THP), 1.64−1.45 (m, 8H, ArCH$_2$CH_2, CH_2CH$_2$OTHP and 4H of THP), 1.39−1.22 (m, 28H, $(CH_2)_{14}$). Anal. ($C_{29}H_{49}IO_2$) C, H.

Tetrahydro-2-[15-(*p*-iodophenyl)pentadecyloxy]-2*H*-pyran (19). This compound was obtained in a manner analogous to that of compound **21** from tosylate **18** (300 mg, 0.55 mmol) and bromide **14** (136 mg, 0.61 mmol). Silica gel chromatography performed as described above gave the product **19** (165 mg, 52%). ^{1}H NMR (360 MHz, $CDCl_3$): 7.58 and 6.92 (2 dt, 2H each, IC_6H_4), 4.59−4.57 (m, 1H, anomeric 2-H of THP), 3.91−3.84 (m, 1H, 6-H_{eq} of THP), 3.73 (dt, 1H, CH_AH$_B$OTHP), 3.54−3.46 (m, 1H, 6-H_{ax} of THP), 3.38 (dt, 1H, CH$_A$$H_B$OTHP), 2.55 (t, 2H, Ar$CH_2$), 1.82−1.67 (m, 2H, THP), 1.64−1.45 (m, 8H, ArCH$_2$CH_2, CH_2CH$_2$OTHP and 4H of THP), 1.39−1.22 (m, 22H, $(CH_2)_{11}$). Anal. ($C_{26}H_{43}IO_2$) C, H.

15-(*p*-Iodophenyl)pentadecanol (20). Compound **19** (150 mg, 0.26 mmol) was converted to the desired product by the procedure described for **17**. Alcohol **20** was obtained in a yield of 91%. ^{1}H NMR (360 MHz, $CDCl_3$): 7.57 and 6.92 (2 dt, 2H each, IC_6H_4), 3.64 (t, 2H, CH_2OH), 2.54 (t, 2H, ArCH_2), 1.60−1.55 (m, 4H, ArCH$_2$CH_2 and CH_2CH$_2$OH), 1.35−1.22 (m, 22H, $(CH_2)_{11}$). Anal. ($C_{21}H_{35}IO$) C, H.

18-(*p*-Iodophenyl)octadecanol (22). By the procedure described for **17**, THP ether **21** (1.4 g, 2.5 mmol) was converted to the desired product **22** in 85% yield. Mp: 72−73 °C (from acetonitrile). ^{1}H NMR ($CDCl_3$) 7.58 and 6.92 (2 dt, 2H each, IC_6H_4), 3.64 (t, 2H, CH_2OH), 2.54 (t, 2H, ArCH_2), 1.60−1.55 (m, 4H, ArCH$_2$CH_2 and CH_2CH$_2$OH), 1.35−1.20 (m 28H, $(CH_2)_{14}$). Anal. ($C_{24}H_{41}IO$) C, H.

18-(*p*-Iodophenyl)octadecyl Methanesulfonate (24). To a solution of 18-(*p*-iodophenyl)octadecanol **22** (150 mg, 0.317 mmol) and triethylamine (0.07 mL, 0.48 mmol) in methylene chloride (2 mL) was added methanesulfonyl chloride (0.03 mL, 0.38 mmol) at 0 °C. Stirring was continued for 40 min, whereupon the reaction mixture was quenched by addition of water. The reaction mixture was diluted with chloroform and washed several times with $NaHCO_3$ solution and water. The chloroform layer was dried over Na_2SO_4 and the solvent was removed in vacuo. The residue was chromatographed with hexane−ethyl acetate (9:1) to afford pure **24** (142 mg, 82%). Mp: 61−62 °C (from ethanol). ^{1}H NMR (360 MHz, $CDCl_3$): 7.58 and 6.92 (2 dt, 2H each, IC_6H_4), 4.22 (t, 2H, CH_2OMs), 3.00 (s, 3H, CH_3S), 2.53 (t, 2H, ArCH_2), 1.75 (quintet, 2H, CH_2CH$_2$OMs), 1.60−1.5 (m, 2H, ArCH$_2$CH_2), 1.40−1.20 (m, 28H, $(CH_2)_{14}$). Anal. ($C_{25}H_{43}IO_3S$) C, H.

15-(*p*-Iodophenyl)pentadecyl Methanesulfonate (23). By the above procedure, alcohol **20** (150 mg, 0.35 mmol) was converted to the desired product **23** (163 mg, 92%). ^{1}H NMR (360 MHz, $CDCl_3$): 7.58 and 6.92 (2 dt, 2H each, IC_6H_4), 4.22 (t, 2H, CH_2-OMs), 3.00 (s, 3H, CH_3S), 2.53 (t, 2H, ArCH_2), 1.75 (quintet, 2H, CH_2CH$_2$OMs), 1.60−1.50 (m, 2H, ArCH$_2$CH_2), 1.40−1.20 (m, 22H, $(CH_2)_{11}$). Anal. ($C_{22}H_{37}IO_3S$) C, H.

1-*O*-[18-(*p*-Iodophenyl)octadecyl]-3-*O*-benzyl-1,3-propanediol (29). Sodium hydride (8 mg of 60% suspension in oil, 0.2 mmol) was added at room temperature to a solution of 3-benzyloxypropanol **25** (0.03 mL, 0.18 mmol) and 18-(*p*-iodophenyl)-octadecyl methanesulfonate **24** (66 mg, 0.12 mmol) in dimethylformamide (3 mL). The reaction mixture was stirred for 12 h, quenched with water, and extracted with ethyl acetate. The extract was washed with brine and dried over Na_2SO_4, and the solvent was removed in a vacuum. Column chromatography with hexane−ethyl acetate (gradient from 95:5 to 85:15) afforded **29** (60 mg; 81%). ^{1}H NMR (360 MHz, $CDCl_3$): 7.58 and 6.92 (2 dt, 2H each, IC_6H_4), 7.36−7.30 (m, 5H, C_6H_5), 4.50 (s, 2H, PhCH_2), 3.57 (t, 2H, alkyl-OCH_2(CH$_2$)$_2$O), 3.52 (t, 2H, CH_2OBn), 3.39 (t, 2H, CH_2O(CH$_2$)$_3$OBn), 2.53 (t, 2H, ArCH_2), 1.90 (quintet, 2H, OCH$_2$CH_2CH$_2$O), 1.65−1.55 (m, 4H, ArCH$_2$CH_2 and CH_2CH$_2$O-(CH$_2$)$_3$O), 1.35−1.20 (m, 28H, (CH$_2$)$_{14}$). Anal. ($C_{34}H_{53}IO_2$) C, H.

1-*O*-[15-(*p*-Iodophenyl)pentadecyl]-3-*O*-benzyl-1,3-propanediol (27). This compound was synthesized as described above from mesylate **23** (85 mg, 0.17 mmol) and 3-benzyloxypropanol **25** (0.036 mL, 0.23 mmol). The compound **27** was obtained in a yield of 79% (76 mg) after chromatographic purification. ^{1}H NMR (360 MHz, $CDCl_3$): 7.58 and 6.92 (2 dt, 2H each, IC_6H_4), 7.36−7.30 (m, 5H, C_6H_5), 4.50 (s, 2H, PhCH_2), 3.57 (t, 2H, alkyl-OCH_2-(CH$_2$)$_2$O), 3.52 (t, 2H, CH_2OBn), 3.39 (t, 2H, CH_2O(CH$_2$)$_3$)OBn), 2.53 (t, 2H, ArCH_2), 1.89 (quintet, 2H, OCH$_2$CH_2CH$_2$O), 1.65−1.55 (m, 4H, ArCH$_2$CH_2 and CH_2CH$_2$O(CH$_2$)$_3$O), 1.40−1.20 (m, 22H, (CH$_2$)$_{11}$). Anal. ($C_{31}H_{47}IO_2$) C, H.

1-*O*-[15-(*p*-Iodophenyl)pentadecyl]-2-*O*-methyl-3-*O*-benzyl-*rac*-glycerol (28). This compound was synthesized as described for **29** from mesylate **23** (92 mg, 0.18 mmol) and 1-*O*-benzyl-2-*O*-methyl-*rac*-glycerol **26**[16] (43 mg, 0.22 mmol) to give 75 mg (68%) of the product. ^{1}H NMR (360 MHz, $CDCl_3$): 7.58 and 6.92 (2 dt, 2H each, IC_6H_4), 7.35−7.25 (m, 5H, C_6H_5), 4.55 (s, 2H, PhCH_2), 3.60−3.50 (m, 5H, CH$_2$CHCH$_2$), 3.45 (s, 3H, OCH$_3$), 3.42 (t, 2H, CH_2OCH$_2$CH), 2.53 (t, 2H, IC$_6$H$_4$CH_2), 1.60−1.50 (m, 4H, ArCH$_2$CH_2 and CH_2CH$_2$O), 1.35−1.20 (m, 22H, (CH$_2$)$_{11}$). Anal. ($C_{32}H_{49}IO_3$), C, H.

1-*O*-[18-(*p*-Iodophenyl)octadecyl]-2-*O*-methyl-3-*O*-benzyl-*rac*-glycerol (30). This compound was synthesized as described for **29** from mesylate **24** (67 mg, 0.12 mmol) and 1-*O*-benzyl-2-*O*-methyl-*rac*-glycerol **26**[16] (36 mg, 0.18 mmol) to give 62 mg (78%) of the product. ^{1}H NMR (360 MHz, $CDCl_3$): 7.58 and 6.92 (2 dt, 2H each, IC_6H_4), 7.35−7.25 (m, 5H, C_6H_5), 4.55 (s, 2H, PhCH_2), 3.60−3.50 (m, 5H, CH$_2$CHCH$_2$), 3.45 (s, 3H, OCH$_3$), 3.42 (t, 2H, CH_2-OCH$_2$CH), 2.53 (t, 2H, IC$_6$H$_4$CH_2), 1.60−1.50 (m, 4H, ArCH$_2$CH_2 and CH_2CH$_2$O), 1.35−1.20 (m, 28H, (CH$_2$)$_{14}$). Anal. ($C_{35}H_{55}IO_3$) C, H.

1-*O*-[18-(*p*-Iodophenyl)octadecyl]-1,3-propanediol (33). Powdered aluminum chloride (353 mg, 2.66 mmol) was added at room temperature to a solution of benzyl ether **29** (413 mg, 0.66 mmol) and anisole (0.36 mL, 3.33 mmol) in methylene chloride (10 mL). Stirring was continued for 2 h. The reaction mixture was quenched by dilution with 1 N HCl, and the aqueous layer was extracted with ethyl acetate. The organic layer was washed with $NaHCO_3$ solution, dried over Na_2SO_4, and evaporated. The remaining residue was chromatographed with hexane−ethyl acetate (gradient from 95:5 to 80:20) to give the product (301 mg, 85%). ^{1}H NMR (360 MHz, $CDCl_3$): 7.58 and 6.92 (2 dt, 2H each, IC_6H_4), 3.78 (q, 2H, CH_2OH), 3.62 (t, 2H, OCH_2CH$_2$CH$_2$OH), 3.42 (t, 2H, CH_2O(CH$_2$)$_3$-OH), 2.55 (t, 2H, ArCH_2, 2H), 1.83 (quintet, 2H, OCH$_2$CH_2CH$_2$-OH), 1.60−1.50 (m, 4H, ArCH$_2$CH_2 and CH_2CH$_2$O(CH$_2$)$_3$OH), 1.35−1.20 (m, 28H, (CH$_2$)$_{14}$). Anal. ($C_{27}H_{47}IO_2$) C, H.

1-*O*-[15-(*p*-Iodophenyl)pentadecyl]-1,3-propanediol (31). By the above procedure, benzyl ether **27** (76 mg, 0.13 mmol) was converted to the alcohol **31** (60 mg, 94%). ^{1}H NMR (360 MHz, $CDCl_3$): 7.58 and 6.92 (2 dt, 2H each, IC_6H_4), 3.78 (q, 2H, CH_2-OH), 3.62 (t, 2H, OCH_2CH$_2$CH$_2$OH), 3.42 (t, 2H, CH_2O(CH$_2$)$_3$-OH), 2.55 (t, 2H, ArCH$_2$), 1.83 (quintet, 2H, OCH$_2$CH_2CH$_2$OH), 1.60−1.45 (m, 4H, ArCH$_2$CH_2 and CH_2CH$_2$O(CH$_2$)$_3$OH), 1.35−1.20 (m, 22H, (CH$_2$)$_{11}$). Anal. ($C_{24}H_{41}IO_2$) C, H.

1-*O*-[15-(*p*-Iodophenyl)pentadecyl]-2-*O*-methyl-*rac*-glycerol (32). Compound **28** (75 mg, 0.12 mmol) was converted to the alcohol **32** (51 mg, 80%) by the procedure described for **33**. ^{1}H NMR (360 MHz, $CDCl_3$): 7.58 and 6.92 (2 dt, 2H each, IC_6H_4), 3.76 and 3.65 (2 m, 2H, CH_2OH), 3.54 (m, 2H, CHCH_2OCH$_2$), 3.47 (s, 3H, OCH$_3$), 3.46−3.41 (m, 3H, CHCH$_2$OCH_2), 2.53 (t, 2H, ArCH_2), 1.60−1.50 (m, 4H, ArCH$_2$CH_2 and OCH$_2$CH_2), 1.35−1.20 (m, 22H, (CH$_2$)$_{11}$). Anal. ($C_{25}H_{43}IO_3$) C, H.

1-*O*-[18-(*p*-Iodophenyl)octadecyl]-2-*O*-methyl-*rac*-glycerol (34) was synthesized as described for **33** from the benzyl ether **30** (58 mg, 0.09 mmol). The alcohol **34** was obtained in a yield of 80% (40 mg). ^{1}H NMR (360 MHz, $CDCl_3$): 7.58 and 6.92 (2 dt, 2H each, IC_6H_4), 3.76 and 3.65 (2 m, 2H, CH_2OH), 3.54 (m, 2H, CHCH_2OCH$_2$), 3.47 (s, 3H, OCH$_3$), 3.46−3.41 (m, 3H, CHCH$_2$-OCH_2), 2.53 (t, 2H, ArCH$_2$), 1.60−1.50 (m, 4H, ArCH$_2$CH_2 and OCH$_2$CH_2), 1.35−1.20 (m, 28H, (CH$_2$)$_{14}$). Anal. ($C_{28}H_{49}IO_3$) C, H.

18-(*p*-Iodophenyl)octadecylphosphocholine (6). 2-Chloro-2-oxo-1,3,2-dioxaphospholane (0.025 mL, 0.27 mmol) was added to the stirred solution of 18-(*p*-iodophenyl)octadecanol **22** (115 mg; 0.24 mmol) in benzene (3 mL) containing triethylamine (0.042 mL, 0.29 mmol). Stirring was continued overnight. The precipitated triethylamine hydrochloride was filtered off and the solvent was removed in vacuo. The residue was transferred into a pressure bottle. A solution of trimethylamine in acetonitrile (5 mL; 25% w/v) was added. The bottle was sealed and heated at 75 °C for 24 h. The acetonitrile was then evaporated and the residue was chromatographed on silica gel with chloroform−methanol (gradient from 10:0 to 5:5) followed by final elution with chloroform−methanol−water (65:25:4). After evaporation of the solvent, the product was precipitated by addition of acetone to give a white solid (130 mg, 84%). ^{1}H NMR (500 MHz, $CDCl_3$−CD_3OD−D_2O 1:1:0.3): 7.59 and 6.96 (2 dt, 2H each, IC_6H_4), 4.28 (br m, 2H, POCH_2CH$_2$N), 3.89 (q, 2H, CH_2OPOCH$_2$CH$_2$N), 3.65 (m, 2H, CH$_2$N), 3.21 (s, 9H, N(CH$_3$)$_3$), 2.57 (2H, t, ArCH_2), 1.68−1.56 (m, 4H, ArCH$_2$CH_2 and CH_2CH$_2$O), 1.40−1.25 (m, 28H, (CH$_2$)$_{14}$). ^{13}C NMR (100 MHz, $CDCl_3$−CD_3OD−D_2O 1:1:0.3): 143.00, 137.63, 131.00, 90.67, 66.73 (d, J_{C-P} = 5.8 Hz), 66.7 (m), 59.60 (d, J_{C-P} = 5.0 Hz), 54.42 (t, J_{C-N} = 3.9 Hz), 35.76, 31.66, 31.09 (d, J_{C-P} = 7.3 Hz), 30.12 (3C), 30.11, 30.08 (2C), 30.05, 30.01, 29.98, 29.89, 29.86, 29.79, 29.48, 26.12. ^{31}P NMR (161.8 MHz, $CDCl_3$−CD_3OD−D_2O 1:1:0.3): 0.80. HRMS: calculated for $C_{29}H_{54}INO_4P$ (M^+ + H) 638.2835, found 638.2828. Anal. ($C_{29}H_{53}INO_4P$), C, H, N, I.

15-(*p*-Iodophenyl)pentadecylphosphocholine (5). The introduction of the phosphocholine moiety into **20** (232 mg, 0.54 mmol) was carried out as described for **6**, yielding **5** (231 mg, 72%) as an amorphous powder. ^{1}H NMR (360 MHz, $CDCl_3$−CD_3OD−D_2O 1:1:0.3): 7.57 and 6.94 (2 dt, 2H each, IC_6H_4), 4.24 (br m, 2H, POCH_2CH$_2$N), 3.85 (q, 2H, CH_2OPOCH$_2$CH$_2$N), 3.61 (m, 2H, CH$_2$N), 3.21 (s, 9H, N(CH$_3$)$_3$), 2.55 (t, 2H, ArCH$_2$), 1.65−1.55 (m, 4H, ArCH$_2$CH_2 and CH_2CH$_2$O), 1.35−1.25 (m, 22H, (CH$_2$)$_{11}$). Anal. ($C_{26}H_{47}INO_4P$) C, H, N.

1-*O*-[15-(*p*-Iodophenyl)pentadecyl]-1,3-propanediol-3-phosphocholine (7). Alcohol **31** (60 mg, 0.12 mmol) was converted into the phosphocholine **7** (65 mg, 81%) as described above for **6**. ^{1}H NMR (360 MHz, $CDCl_3$−CD_3OD−D_2O 1:1:0.3): 7.57 and 6.94 (2 dt, 2H each, IC_6H_4), 4.26 (br m, 2H, POCH_2CH$_2$N), 3.93 (q, 2H, CH_2OPOCH$_2$CH$_2$N), 3.61 (m, 2H, CH$_2$N), 3.54 (t, 2H, OCH_2-CH$_2$CH$_2$OP), 3.21 (s, 9H, N(CH$_3$)$_3$), 2.55 (t, 2H, ArCH_2), 1.65−1.55 (m, 4H, ArCH$_2$CH_2 and CH_2CH$_2$O(CH$_2$)$_3$OP), 1.35−1.25 (m, 28H, (CH$_2$)$_{14}$). Anal. ($C_{29}H_{53}INO_5P$) C, H, N.

1-*O*-[15-(*p*-Iodophenyl)pentadecyl]-2-*O*-methyl-*rac*-glycero-3-phosphocholine (9). Using procedure for the synthesis of **6**, alcohol **32** (51 mg, 0.1 mmol) was converted into the phosphocholine **9** (55 mg, 82%). ^{1}H NMR (360 MHz, $CDCl_3$−CD_3OD−D_2O 1:1:0.3): 7.57 and 6.95 (2 dt, 2H each, IC_6H_4), 4.26 (br m, 2H, POCH_2-CH$_2$N), 3.95 and 3.86 (2 m, 2H, CHCH_2OP), 3.62 (m, 2H, CH$_2$N), 3.60−3.50 (m, 3H, CHCH$_2$OCH$_2$), 3.47 (s, 3H, OCH$_3$), 3.46 (t, 2H, CHCH$_2$OCH_2), 3.21 (s, 9H, N(CH$_3$)$_3$), 2.55 (t, 2H, ArCH_2), 1.65−1.55 (m, 4H, ArCH$_2$CH_2 and CH_2CH$_2$OCH$_2$), 1.35−1.22 (m, 22H, m, (CH$_2$)$_{11}$). Anal. ($C_{30}H_{55}INO_6P$) C, H, N.

1-*O*-[18-(*p*-Iodophenyl)octadecyl]-1,3-propanediol-3-phosphocholine (8). The phosphocholine **8** was synthesized by an analogous manner to that of **6** from the alcohol **33** (42 mg; 79 mmol) in 55% yield (45 mg). ^{1}H NMR (360 MHz, $CDCl_3-CD_3OD-D_2O$ 1:1:0.3): 7.57 and 6.94 (2 dt, 2H each, IC_6H_4), 4.26 (br m, 2H, $POCH_2CH_2N$), 3.93 (q, 2H, $CH_2OPOCH_2CH_2N$), 3.61 (m, 2H, CH_2N), 3.54 (t, 2H, $OCH_2CH_2CH_2OP$), 3.21 (s, 9H, $N(CH_3)_3$), 2.55 (t, 2H, $ArCH_2$), 1.65−1.55 (m, 4H, $ArCH_2CH_2$ and $CH_2CH_2O(CH_2)_3OP$), 1.35−1.25 (m, 28H, $(CH_2)_{14}$). Anal. ($C_{32}H_{59}INO_5P$) C, H, N.

1-*O*-[18-(*p*-Iodophenyl)octadecyl]-2-*O*-methyl-*rac*-glycero-3-phosphocholine (10). The phosphocholine **10** was synthesized from the alcohol **34** (33 mg, 0.06 mmol) by the procedure described above for **6** in a yield of 75% (32 mg). ^{1}H NMR (360 MHz, $CDCl_3-CD_3OD-D_2O$ 1:1:0.3): 7.57 and 6.95 (2 dt, 2H each, IC_6H_4), 4.26 (br m, 2H, $POCH_2CH_2N$), 3.95 and 3.86 (2 m, 2H, $CHCH_2OP$), 3.62 (m, 2H, CH_2N), 3.60−3.50 (m, 3H, $CHCH_2OCH_2$), 3.47 (s, 3H, OCH_3), 3.46 (t, 2H, $CHCH_2OCH_2$), 3.21 (s, 9H, $N(CH_3)_3$), 2.55 (t, 2H, $ArCH_2$), 1.65−1.55 (m, 4H, $ArCH_2CH_2$ and $CH_2CH_2OCH_2$), 1.35−1.22 (m, 28H, m, $(CH_2)_{14}$). Anal. ($C_{33}H_{61}INO_6P$) C, H, N.

Radioiodination of Phospholipid Ether Analogues. For the biological studies, 7-(*p*-iodophenyl)heptyl phosphocholine (**3**, NM-396) and 12-(*p*-iodophenyl)dodecyl phosphocholine (**4**, NM-346), whose syntheses have been described previously,[12] have been included for comparison purposes. Radioiodination of the PLE analogues with iodine-125 was accomplished by an isotope exchange reaction as previously reported.[17] Radiochemical purity was established by radio-thin-layer chromatography with unlabeled material serving as a standard. Specific activities for the chain length homologues ranged from 0.08 to 4.0 Ci/mmol. Radiochemical purity exceeded 95% for all labeled compounds.

Biological Studies. Cell Lines and Culture Conditions. Walker 256 carcinosarcoma cells were maintained in RPMI 1640 medium containing 10% fetal bovine serum (FBS), 200 units/mL of penicillin, and 0.2 mg/mL streptomycin. Cells were maintained at 37 °C in a humidified atmosphere of 5% CO_2.

Animals. All procedures using animals conformed strictly to the guidelines set forth by the animal care units of each respective institution, which reviewed and approved the experimental protocol. Female Sprague−Dawley rats (200−250 g from Charles River, Portage, Michigan) were housed in a temperature- and light-controlled room and had free access to food and water. The rats were inoculated with Walker 256 carcinosarcoma cells (5.0×10^6 cells) in 0.2 mL of saline in the right hind limb. Tumors were allowed to develop for 7−14 days prior to injection with PLE analogues.

Male Copenhagen rats (200−220 g, Harlan) were housed under the same conditions. The rats were inoculated subcutaneously with MAT LyLu prostate cancer cells (1.0×10^6 cells) in 0.1 mL of phosphate-buffered saline in the right hind limb. Tumors were permitted to grow for 10−14 days prior to initiation of γ-camera imaging with the radioiodinated PLE homologues (30−50 μCi, iv).

Male SCID mice (19−22 g, Harlan) were housed in a temperature- and light-controlled room and had free access to food and water. Each was inoculated with human PC-3 prostate tumor cells (5×10^5 cells) in 0.1 mL of saline in the right hind limb. Tumors were allowed to develop 10−14 days prior to injection with ^{125}I-NM-404.

Tissue Distribution. The radiolabeled compounds were dissolved in absolute ethanol, Tween-20 (0.1 mL/mg of compound) was added to this solution, and the solvent was evaporated with a stream of nitrogen. Physiological saline was added, to give a 2−3% Tween-20 solution. The solubilized radiolabeled compound (5−10 μCi in 0.3 mL or 2−5 μCi in 0.2 mL) was administered intravenously via tail vein to tumor-bearing rats or mice, respectively. Injected dose was normalized to the mass of radiolabeled compound and body weight of the recipient in order to maintain consistency of injected mass dose between animals in comparative studies. The animals were euthanized by exsanguination while under anesthesia at the various time points. Blood was collected and selected tissues were removed and blotted to remove excess blood. Large organs were minced with scissors. Tissue samples were weighted in gelatin capsules and counted with a Searle-1185 well scintillation counter (88% counting efficiency). The concentration of radioactivity in each tissue was expressed as a percentage of administered dose per gram of tissue.

Due to its production of thyroxine hormones, the thyroid gland is the major site of accumulation of free iodide ion found in the plasma. Sequestration of plasma iodide is so efficient that $Na^{131}I$ is administered orally for thyroid ablation. Thyroid radioactivity following injection of radioiodinated radiopharmaceuticals has been used as an indicator of in vivo deiodination in nuclear medicine for many years. In fact, in most clinical trials with these agents, patients receive an oral dose of saturated potassium iodine solution in order to presaturate the thyroid and thus minimize subsequent uptake of free radioiodide. In our own clinical trial, presaturation with saturated potassium iodine solution would not be expected to effect thyroid activity, if uptake was due to intact PLE analogue and not to free iodide. Our results showing no subsequent thyroid radioactivity confirmed the in vivo stability toward deiodination and direct uptake of the PLE analogue into the thyroid.

γ-Camera Scintigraphy. The radiolabeled compounds were dissolved in absolute ethanol (50−500 μL), and Tween-20 (0.1 mL/mg of compound) was added to the solution. Ethanol was removed by evaporation under a stream of nitrogen. Normal saline was added, to give a 2−3% Tween-20 solution, which was subsequently mixed by vortex. The solubilized radiolabeled compound (35−50 μCi, 0.5 mL per rat; 10−15 μCi, 0.2 mL per mouse) was administered intravenously via tail vein to anesthetized tumor-bearing animals ($n \geq 3$ per time point). Scanning of the animals was performed using an LEM Mobile Camera, Siemens Corp. (Hoffman Estates, IL) with a high-sensitivity−low-energy collimator window optimized for the low-energy γ-emissions of iodine-125. Image acquisition and storage was accomplished with a Siemens MicroDELTA computer connected to a larger MicroVAX unit. Animals ($n = 2$ per compound) were sedated with a premixed solution 87 mg/kg ketamine and 13 mg/kg xylazine. Images were accumulated for 20 min at various times (1, 3, 6, and 24 h and at 24-h intervals thereafter to 120 h) following tail-vein administration of radiolabeled compound (40−50 μCi, 0.5−1.0 mL). Animals were euthanized after imaging protocols and were subjected to tissue distribution analysis.

The human ^{131}I-NM-404 (800 μCi) images were acquired on a GE Maxxus dual-head SPECT imaging system using a whole body scanning protocol at 1, 2, and 4 days after intravenous administration.

Acknowledgment. The authors wish to thank Dr. James Varani of the Department of Pathology, University of Michigan Medical School, for providing the Walker 256 carcinosarcoma cells and Dr. Ken Pienta, Department of Urology, University of Michigan Medical School, for providing the prostate tumor-bearing rats and mice. The authors wish to acknowledge Dr. Thomas C. Stringfellow and Mr. Gary Girdaukas of the Analytical Instrumentation Center in the University of Wisconsin, School of Pharmacy, for assistance in obtaining NMR and mass spectra, respectively. Support for this research was provided by the National Institute of Health grants CA-08349 (R.E.C.) and CA-92412 (J.P.W.).

References

(1) Snyder, F.; Wood, R. Alkyl and alk-1-enyl ethers of glycerol in lipids from normal and neoplastic human tissues. *Cancer Res.* **1969**, *29*, 251−257.

(2) Snyder, F.; Blank, M. L.; Morris, H. P. Occurrence and nature of *O*-alkyl and *O*-alk-1-enyl moieties of glycerol in lipids of Morris transplanted hepatomas and normal rat liver. *Biochim. Biophys. Acta* **1969**, *176*, 502−510.

(3) Soodsma, J. F.; Piantadosi, C.; Snyder, F. The biocleavage of alkyl glyceryl ethers in Morris hepatomas and other transplantable neoplasms. *Cancer. Res.* **1970**, *30*, 309−311.

(4) Lee, T. C.; Blank, M. L.; Fitzgerald, U.; Snyder, F. Substrate specificity in the biocleavage of the *O*-alkyl bond: 1-Alkyl-2-acetyl-*sn*-glycero-3-phosphocholine (a hypotensive and platelet-activating lipid) and its metabolites. *Arch. Biochem. Biophys.* **1981**, *208*, 353−357.
(5) For review, see: Gajate, C.; Mollinedo, F. Biological activities, mechanisms of action and biomedical prospect of the antitumor ether phospholipid ET-18-OCH_3 (edelfosine), a proapoptotic agent in tumor cells. *Curr. Drug Metab.* **2002**, *3*, 491−525.
(6) Wahl, R. L.; Fig, L. M.; Zasadny, K. R.; Gross, M. D.; Weichert, J. P.; Counsell, R. E. Initial clinical evaluation of I-131 NM-324, a tumor-avid phospholipid ether, in humans with cancer. *Radiology*. **1997**, *205* (P), 478, Abstract 1429.
(7) Meyer, K. L.; Schwendner, S. W.; Counsell, R. E. Potential tumor or organ imaging agents. 30. Radioiodinated phospholipid ethers. *J. Med. Chem.* **1989**, *32*, 2142−2147.
(8) Counsell, R. E.; Schwendner, S. W.; Meyer, K. L.; Haradahira, T.; Gross, M. D. Tumor visualization with a radioiodinated phospholipid ether. *J. Nucl. Med.* **1990**, *31*, 332−336.
(9) Plotzke, K. P.; Haradahira, T.; Stancato, L.; Olken, N. M.; Skinner, R. W. S.; Gross, M. D.; Wahl, R. L.; Counsell, R. E. Selective localization of radioiodinated alkylphosphocholine derivatives in tumors. *Nucl. Med. Biol.* **1992**, *19*, 765−773.
(10) Plotzke, K. P.; Fisher, S. J.; Wahl, R. L.; Olken, N. M.; Skinner, R. W. S.; Gross, M. D.; Counsell, R. E. Selective localization of a radioiodinated phospholipid ether analog in human tumor xenografts. *J. Nucl. Med.* **1993**, *34*, 787−792.
(11) Plotzke, K. P.; Rampy, M. A.; Meyer, K.; Ruyan, M.; Fisher, S. J.; Wahl, R. L.; Skinner, R. W. S.; Gross, M. D.; Counsell, R. E. Biodistribution, metabolism, and excretion of radioiodinated phospholipid ether analogs in tumor-bearing rats. *J. Nucl. Biol. Med*. **1993**, *37*, 264−272.
(12) Rampy, M. A.; Chou, T. S.; Pinchuk, A. N.; Skinner, R. W. S.; Gross, M. D.; Fisher, S.; Wahl, R. L.; Counsell, R. E. Synthesis and biological evaluation of radioiodinated phospholipid ether analogs. *Nucl. Med. Biol.* **1995**, *22*, 505−512.
(13) Rampy, M. A.; Pinchuk, A. N.; Weichert, J. P.; Skinner, R. W. S.; Fisher, S. J.; Wahl, R. L.; Gross, M. D.; Counsell, R. E. Synthesis and biological evaluation of radioiodinated phospholipid ether stereoisomers. *J. Med. Chem*. **1995**, *38*, 3156−3162.
(14) Rampy, M. A.; Brown, R. S.; Pinchuk, A. N.; Weichert, J. P.; Skinner, R. W. S.; Fisher, S. J.; Wahl, R. L.; Gross, M. D.; Ethier, S. P.; Counsell, R. E. Biological disposition and imaging of a radioiodinated alkylphosphocholine in two rodent models of breast cancer. *J. Nucl. Med*. **1996**, *37*, 1540−1545.
(15) (a) Fouquet, G.; Schlosser, M. Improved carbon−carbon linking by controlled copper catalysis. *Angew. Chem. Int. Ed.* **1974**, *13*, 82−83. (b) Schlosser, M.; Bossert, H. The "two-fold reaction" benchmark applied to the copper catalyzed assembling of 1,ω-difunctional hydrocarbon chains. *Tetrahedron* **1992**, *47*, 6287−6292. (c) A review on metal-catalyzed cross-coupling of Grignard reagents: Urabe, H.; Sato, F. Metal-catalyzed reactions. In *Handbook of Grignard Reagents*; Silverman, G. S., Rakita, P. E., Eds.; Marcel Dekker: New York, 1996; pp 577−632.
(16) Pinchuk, A. N.; Mitsner, B. I.; Shvets, V. I. 1-*O*-Benzyl-2-*O*-methyl-*rac*-glycerol: A key intermediate for synthesis of ether glycerolipids. *Chem. Phys. Lipids* **1991**, *59*, 263−265.
(17) Weichert, J. P.; VanDort, M. E.; Groziak, M. P.; Counsell, R. E. Radioiodination via isotope exchange in pivalic acid. *Appl. Radiat. Isotop.* **1986**, *37*, 907−913.
(18) Kötting, J.; Marschner, N. W.; Neumüller, W.; Unger, C.; Eibl, H. Hexadecylphosphocholine and octadecyl-methyl-glycero-3-phosphocholine: A comparison of hemolytic activity, serum binding and tissue distribution. In *Progress in Experimental Tumor Research*; Eibl, H., Hilgard, P., Unger, C., Eds.; Karger: Basel, Switzerland, 1992; Vol. 34, pp 131−142.
(19) Kötting, J.; Berger, M. R.; Unger, C.; Eibl, H. Alkylphosphocholines: Influence of structural variation and biodistribution at antineoplastically active concentrations. *Cancer Chemother. Pharmacol.* **1992**, *30*, 105−112.
(20) Blasberg, R. G.; Roelcke, U.; Weinreich, R.; Beattie, B.; von Ammon, K.; Yonekawa, Y.; Landolt, H.; Guenther, I.; Crompton, N. E. A.; Vontobel, P.; Missimer, J.; Maguire, R. P.; Koziorowski, J.; Knust, E. J.; Finn, R. D.; Leenders, K. L. Imaging brain tumor proliferative activity with [I-124]iododeoxyuridine. *Cancer Res*. **2000**, *60*, 624−635.
(21) Pentlow, K. S.; Graham, M. C.; Lambrecht, R. M.; Daghighian, F.; Bacharach, S. L.; Bendriem, B.; Finn, R. D.; Jordan, K.; Kalaigian, H.; Karp, J. S.; Robeson, W. R.; Larson, S. M. Quantitative imaging of iodine-124 with PET. *J. Nucl. Med*. **1996**, *37*, 1557−1562.

JM050252G